

Neutron Reflectivity Studies of the Adsorption of Aerosol-OT at the Air–Water Interface: The Structure of the Sodium Salt

Z. X. Li, J. R. Lu, and R. K. Thomas*

Physical and Theoretical Chemistry Laboratory, South Parks Road, Oxford OX1 3QZ, UK

J. Penfold

ISIS, DRAL, Chilton, Didcot, Oxon, OX11 0QX, UK

Received: September 11, 1996; In Final Form: December 27, 1996[⊗]

We have combined neutron reflection measurements with isotopic substitution to determine the structure of a layer of sodium *bis*(2-ethyl-1-hexyl)sulfosuccinate (aerosol-OT or AOT) adsorbed at the air/solution interface. The widths of the distributions of the upper and lower halves of the molecule, as well as their positions in relation to the underlying water, have been measured at four concentrations varying from the critical micelle concentration (cmc) (2.5×10^{-3} M) to CMC/300. Over this concentration range the coverage changes from 78 ± 3 to 132 ± 8 Å²/molecule but the thickness of the surfactant layer does not change at all, unlike the behavior of all other soluble surfactants so far studied by neutron reflection. At the highest surface coverage we conclude that the butyl chains are strongly tilted away from the surface normal. At the lowest surface coverage the unexpectedly large width of the chain distribution is attributed to the molecule as a whole being tilted in such a way that the two ethyl hexanol fragments are on average at different levels in the interface. The only directly observable change in the layer is that the centers of the distributions of the two halves of the molecule move closer to the water as the surface concentration is reduced, suggesting that the molecules become more immersed in the water at low coverages.

Introduction

The anionic surfactant sodium *bis*(2-ethyl-1-hexyl) sulfosuccinate (aerosol-OT or AOT) has been very widely used in research and technological applications, for example, in ref 1. In common with most other surfactants little is known about its structure at interfaces because of a general lack of experimental techniques capable of probing wet interfaces. We have started using the relatively new technique of neutron reflection to study the structural characteristics of AOT layers at the liquid/air² and solid/liquid³ interfaces. In particular we wish to identify whether there are any special structural characteristics of AOT layers that can be identified such as, for example, the roughness of the layer, the degree of immersion of the surfactant in the water, and the conformation of the two branched chains, and we have already shown for other surfactants that all of these features are accessible to neutron reflection (see ref 4). In a previous paper we have also used neutron reflection to determine the variation of surface excess with concentration of NaAOT,⁵ and we have published a preliminary study of the structure of AOT at the air/solution interface at its critical micelle concentration (cmc).² Here, we present a more thorough structural study over a range of concentration.

Experimental Details

Protonated AOT ($\text{C}_8\text{H}_{17}\text{OOC})_2\text{C}_2\text{H}_3\text{SO}_3\text{Na}$ (abbreviated to h-AOT) was obtained from *Sigma* and purified by liquid/liquid extraction as described below. Three partially deuteriated surfactants ($\text{C}_4\text{D}_9\text{CD}(\text{C}_2\text{D}_5)\text{CD}_2\text{OOC})_2\text{C}_2\text{H}_3\text{SO}_3\text{Na}$ (abbreviated to dUdL-AOT, *U* and *L* signifying upper and lower chain respectively, and *d* and *h* signifying deuteration or protonation), ($\text{C}_4\text{D}_9\text{CH}(\text{C}_2\text{H}_5)\text{CH}_2\text{OOC})_2\text{C}_2\text{H}_3\text{SO}_3\text{Na}$ (dUhL-AOT), and ($\text{C}_4\text{H}_9\text{CD}(\text{C}_2\text{D}_5)\text{CD}_2\text{OOC})_2\text{C}_2\text{H}_3\text{SO}_3\text{Na}$ (abbreviated to hUdL-AOT)

were synthesized as follows. 2-Ethyl-1-hexanoic acid was synthesized by successive reactions of butyl and ethyl bromide with diethyl malonate using standard procedures.⁶ After decarboxylation of the product, LiAlD_4 was used to reduce the acid to ethyl hexanol. After purification of the ethyl hexanol on a silica gel column using an ether/hexane solvent, the ethyl hexanol was reacted with fumaric acid to give the diester of the acid, from which residual ethylhexanol and monoester were removed on a silica gel column using an ether/hexane mixture. The fumaric acid diester was reacted with an aqueous solution of sodium bisulfite to give the sulfosuccinate AOT.⁷ Residual salt was removed by successive extraction, evaporation, and filtration using methanol.

We purified the AOT following the procedure of Williams *et al.*⁸ but with one modification. The product obtained after extraction with methanol was dissolved in a methanol/water mixture and a liquid/liquid extraction with hexane performed for 24 h to remove any unreacted diester, monoester, or ethylhexanol produced by hydrolysis in the addition step. The modification, which we found improved the extraction, was to hold the AOT solution at 0 °C during the liquid/liquid extraction, which reduces the rate of hydrolysis of the ester groups in the AOT.

Initially the purity was assessed from the surface tension as a function of concentration. No minimum was observed and the CMC was found to be 2.5×10^{-3} M, in good agreement with other measurements.⁹ No differences were observed between the four AOT isotopes when H_2O was the solvent. The surface tension measurements were performed on a Kruss K10 tensiometer using a Pt/Ir ring.

Reflectivity measurements were made on the CRISP neutron reflectometer at the Rutherford Appleton Laboratory, Didcot, UK, using procedures described previously,¹⁰ and all measurements were made at 298 K.

[⊗] Abstract published in *Advance ACS Abstracts*, February 1, 1997.

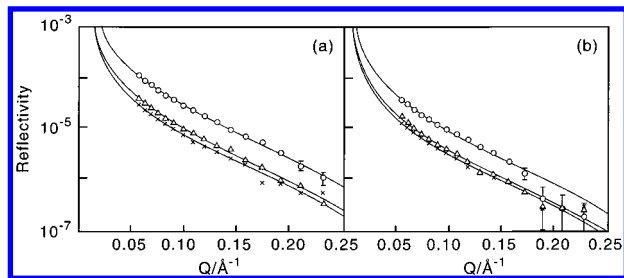


Figure 1. Neutron reflectivity profiles of dUdL-AOT (○), dUhL-AOT (△), and hUdL-AOT (×) in null reflecting water at (a) the cmc (2.5×10^{-3} M) and (b) cmc/300. The reflectivities decrease from dUdL-AOT, dUhL-AOT through to hUdL-AOT. The continuous lines are fits using a single uniform monolayer with the parameters given in Table 1.

TABLE 1: Parameters from One-Layer Model Fitting for the Profiles in NRW

surfactant	concentration	thickness/ Å	$10^6 \rho /$ Å ⁻²	$A / \text{Å}^2$ molecule ⁻¹
dUdL-AOT	cmc	18 ± 1	2.8 ± 0.2	78 ± 4
	cmc/30	17	2.6	90
	cmc/150	18	1.8 ₅	118
	cmc/300	18 ± 3	1.5 ± 0.3	137 ± 10
dUhL-AOT	cmc	18 ± 2	$1.6_5 \pm 0.2$	77 ± 4
	cmc/30	18	1.4	91
	cmc/150	18	1.1	116
	cmc/300	18 ± 4	1.0 ± 0.2	130 ± 10
hUdL-AOT	cmc	18 ± 2	$1.4_5 \pm 0.2$	79 ± 4
	cmc/30	18	1.1	104
	cmc/150	18	0.9 ₅	120
	cmc/300	18 ± 3	0.9 ± 0.2	129 ± 10

Results

The neutron reflectivity profiles for the three isotopic species containing some deuterium in solution in null reflecting water (NRW) are shown for the highest (cmc) and lowest (cmc/300) concentrations in Figure 1 together with the best fits of a uniform monolayer to the data using the optical matrix method of calculation.¹¹ Three parameters are obtained on fitting such a model, the thickness of the labeled fragment, the scattering length density of the layer, and the surface coverage, and these parameters are given for four concentrations in Table 1. We have discussed the coverage in a previous paper,⁵ so here we focus on the structural properties of the layer. There are two unusual features about the results. First, the layer thickness is the same whatever the fragment being highlighted by the reflectivity, and second, the layer thickness does not vary with coverage. The first feature is characteristic of a molecule with smallish extended dimensions and a rough layer. The second feature is unusual in that for all other surfactant layers that we have studied we have found that the layer becomes progressively thinner as the surface coverage decreases. We will comment further after analyzing the structure in more detail.

As we have shown in other papers concerning monolayers of soluble surfactants, it is more natural to interpret reflectivity data using the kinematic approximation and partial structure factors of the different components of the system than to fit the data using a set of uniform monolayers to describe the structure.¹² In large part this is because use of the kinematic approximation incidentally allows more realistic distributions to be used for the different fragments of the layer. In many cases it is possible to use a labeling scheme that unambiguously distinguishes what might be considered to be the distinct parts of the amphiphile, e.g., chains, heads, and water. This is not the case for AOT. The scattering length of the bulky headgroup, which contains two carboxy groups and an SO₃ group, cannot be varied over a wide enough range because it contains only

three exchangeable protons. Our labeling scheme divides the chain into two parts, which we refer to as *U* and *L*, upper and lower chain fragments, and we use *H* to indicate the headgroup and *W* for water. In the kinematic approximation the reflectivity is then

$$R = \frac{16\pi^2}{\kappa^2} [b_U^2 h_{UU} + b_L^2 h_{LL} + b_H^2 h_{HH} + b_W^2 h_{WW} + 2b_U b_L h_{UL} + 2b_U b_H h_{UH} + 2b_U b_W h_{UW} + 2b_L b_H h_{LH} + 2b_L b_W h_{LW} + 2b_H b_W h_{HW}] \quad (1)$$

where h_{ii} are the self-partial structure factors and h_{ij} are the cross terms in the partial structure factors, related to the Fourier transforms of the number density distributions of the fragments by

$$h_{ii} = \kappa^2 |\hat{n}_i(\kappa)|^2 \quad (2)$$

$$h_{ij} = \kappa^2 \text{Re}\{\hat{n}_i(\kappa) \hat{n}_j(\kappa)\} \quad (3)$$

$\hat{n}(\kappa)$ is the Fourier transform of the number density profile and is

$$\hat{n}_i(\kappa) = \int n_i(z) \exp(ikz) dz \quad (4)$$

where $n(z)$ is the number density distribution normal to the interface.

For soluble surfactants, which form a relatively low density layer at the surface, we have found that a Gaussian distribution is a good representation of the number density profile of a layer consisting of a fragment of amphiphile, while water is best represented by a tanh profile. The partial structure factors for these two cases are respectively

$$\kappa^2 h_{ii} = \frac{\kappa^2}{A_i} \exp(-\kappa^2 \sigma_i^2 / 8) \quad (5)$$

where σ_i is the full width of the *i*th layer at $1/e$ of its height and A_i is the area occupied by the fragment, and

$$\kappa^2 h_{ww} = n_{w_0}^2 (\zeta \pi \kappa / 2)^2 \text{cosech}^2(\zeta \pi \kappa / 2) \quad (6)$$

where n_{w_0} is the number density of bulk water and ζ is the width parameter for the tanh profile. The cross partial structure factors can be obtained from the self-partial structure factors using¹³

$$h_{ij} = \pm (h_{ii} h_{jj})^{1/2} \cos \kappa \delta_{ij} \quad (7)$$

$$h_{iw} = \pm (h_{ii} h_{ww})^{1/2} \sin \kappa \delta_{iw} \quad (8)$$

where δ_{ij} is the separation distance of the centers of the layers. We have discussed the circumstances where these approximations fail,^{13,14} but these are not expected to arise for AOT. Further constraints are that

$$\begin{aligned} \delta_{UH} &= \delta_{UL} + \delta_{LH} \\ \delta_{UW} &= \delta_{UL} + \delta_{LW} \\ \delta_{LW} &= \delta_{LH} + \delta_{HW} \end{aligned} \quad (9)$$

Since the scattering length of the headgroup is small relative to either of the deuterated *U* or *L* groups or to D₂O and since its labeling is not altered in the experiment the number of terms in eq 1 can be reduced by combining the lower part of the chain

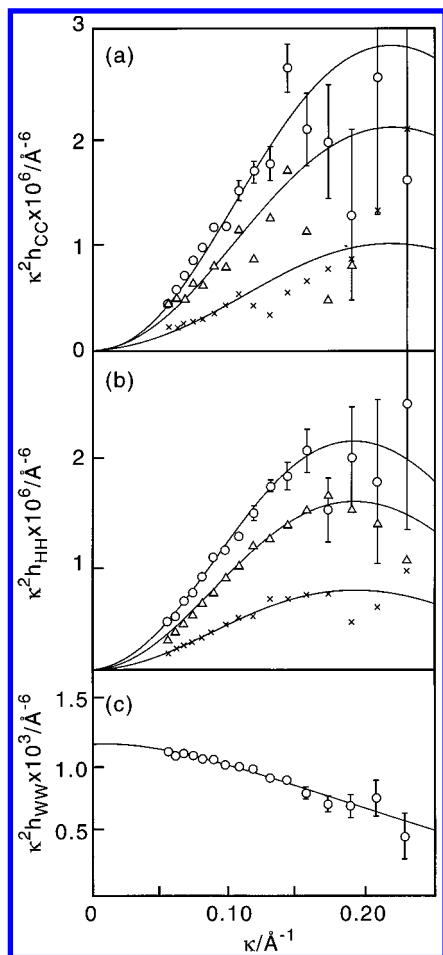


Figure 2. Self-partial structure factors (a) upper chains, (b) heads (h), and (c) water of the AOT layer at three concentrations, (O) cmc (2.5×10^{-3} M), (Δ) cmc/30, and (+) cmc/150. Measurements were made at a fourth concentration but are omitted for clarity. The data for the water structure factor are shown for only one concentration (cmc) for the same reason. The continuous lines are the best fits using the parameters of Table 2.

with the headgroup to give a modified headgroup, which we designate h . This gives an approximate expression for the reflectivity:

$$R = (16\pi^2/\kappa^2)[b_U^2 h_{UU} + b_h^2 h_{hh} + b_W^2 h_{WW} + 2b_U b_h \sqrt{h_{UU} h_{hh}} \cos \kappa \delta_{Uh} + 2b_U b_W \sqrt{h_{UU} h_{WW}} \sin \kappa \delta_{UW} + 2b_h b_W \sqrt{h_{hh} h_{WW}} \sin \kappa \delta_{hW}] \quad (10)$$

where we have made use of eqs 7 and 8. The advantage of this second expression is that it allows an approximate structure to be derived analytically from six reflectivity profiles from suitably labeled species.

We first determine the structure of the layer using the simpler eq 10. To solve eq 10 analytically, six reflectivity profiles of different isotopic composition were required and these were chosen to be dUdL-AOT, dUhL-AOT and hUdL-AOT in NRW, and dUdL-AOT, and dUhL-AOT and hUhL-AOT in D₂O. These data give six simultaneous equations from which the six structure factors in eq 10 can be extracted. The resulting self-structure factors for three of the four concentrations measured are shown in Figure 2 with the best fits using eqs 5 and 6. The cross terms in the partial structure factors are shown in Figure 3 with the best fits using eqs 5 and 6 together with eqs 7 and 8. The best-fit parameters are given in Table 2. The three values of δ are determined independently in this analysis and

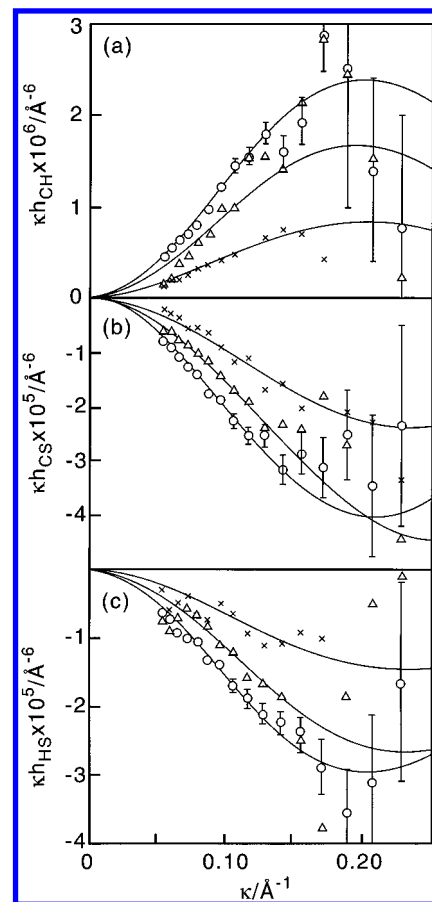


Figure 3. Cross terms in the partial structure factors (a) upper chains/heads, (b) upper chains/water, and (c) heads (h)/water for AOT at three concentrations, (O) cmc (2.5×10^{-3} M), (Δ) cmc/30, and (+) cmc/150. Measurements were made at a fourth concentration but are omitted for clarity. The continuous lines are the best fits using the parameters of Table 2.

satisfy the appropriate condition of the type shown in eq 9 within the error of the experiment.

The difficulty in interpreting the parameters in Table 2 is that any parameters concerning the composite headgroup h , which is the combination of the lower part of the chain and the actual hydrophilic headgroup, are difficult to interpret. The two groups constituting h are expected to be at different levels in the interface, and because the actual headgroup has a lower scattering length than the lower part of the deuterated chain, any parameters involving either L or H will be a weighted average which is not easy to evaluate. The 10 terms in eq 1 suggest that 10 independent measurements may be needed to determine the structure of the layer at a resolution where L and H are distinguished. However, if eqs 7 and 8 are incorporated into eq 1, we obtain

$$R = (16\pi^2/\kappa^2)[b_U^2 h_{UU} + b_L^2 h_{LL} + b_H^2 h_{HH} + b_W^2 h_{WW} + 2b_U b_L \sqrt{h_{UU} h_{LL}} \cos \kappa \delta_{UL} + 2b_U b_H \sqrt{h_{UU} h_{HH}} \cos \kappa \delta_{UH} + 2b_U b_W \sqrt{h_{UU} h_{WW}} \sin \kappa \delta_{UW} + 2b_L b_H \sqrt{h_{LL} h_{HH}} \cos \kappa \delta_{LH} + 2b_L b_W \sqrt{h_{LL} h_{WW}} \sin \kappa \delta_{LW} + 2b_H b_W \sqrt{h_{HH} h_{WW}} \sin \kappa \delta_{HW}] \quad (11)$$

which, because of the relations 9, contains only four unknown self-structure factors and three unknown separations. In any case it is not necessary to measure one reflectivity profile for each unknown parameter of the structure because there is one set of simultaneous equations at each of a large number of values of κ (see Lu et al. for a discussion of this point¹²). Nevertheless,

TABLE 2: Structural Parameters Obtained from the Kinematic Approximation When the Molecule Is Taken To Consist Just of Chain (*U*) and Head (*h*) Fragments

$A/\text{\AA}^2$	$\sigma_U \pm 2/\text{\AA}$	$\sigma_h \pm 2/\text{\AA}$	$\zeta/\text{\AA}$	$\delta_{UW}/\text{\AA}$	$\delta_{UW}/\text{\AA}$	$\delta_{HW}/\text{\AA}$
78 ± 2	13	15	4 ± 1	2 ± 1	6 ± 1	4.5 ± 1
94 ± 3	13	15	3 ± 1.5	2 ± 1	5 ± 1.5	4 ± 1
118 ± 4	13	15	3 ± 1.5	2 ± 1.5	5 ± 2	3.5 ± 1.5
132 ± 5	13	15	3 ± 2	2 ± 2	4.5 ± 2	3 ± 1.5

we have measured an additional seventh reflectivity, that of hUdL-AOT in D₂O. Unfortunately, even with seven reflectivity profiles and seven unknowns the equations cannot be solved analytically because three of the unknowns are arguments of cos or sin functions. We have therefore used a procedure, described by Lee et al.¹⁵ which simultaneously fits the set of reflectivity profiles to eq 11 using a least-squares minimization. The fits to six of the seven reflectivity profiles are shown in Figure 4 for the measurements at the cmc and the parameters obtained for all four concentrations given in Table 3.

It is worth comparing the results in Tables 2 and 3, particularly those involving the groups *H* and *L*. As expected, the weighting of the cross sections when the two groups are combined into one has the effect that the parameters for *h* in Table 2 closely resemble those for *L* in Table 3. This might suggest that the experiment should be relatively incapable of determining any information about the true headgroup *H*. However, when the analysis uses eq 10, the position of the *h* group is largely determined by the reflectivity profile of dUdL-AOT in NRW, but when the analysis uses eq 11, the position of the *H* group is determined mainly by the D₂O profiles where the actual headgroup is highlighted because it displaces the high scattering length D₂O. This is revealed very clearly when doing the fitting using eq 10 because, although the fit is somewhat insensitive to the values of the widths of the three distributions *U*, *L*, and *H*, and these may be varied over a limited range, the values obtained for the three separations are extremely well defined. The situation in AOT is just slightly more complicated than for the non-ionic surfactant C₁₂H₂₅(OC₂H₄)₃OH (abbreviated to C₁₂E₃) where we have shown that the set of structural parameters defining the C₁₂E₃ layer can be determined from just three reflectivity profiles, dC₁₂hE₃ in NRW and hC₁₂hE₃ and dC₁₂hE₃ in D₂O, without any need to deuterate the E₃ group.¹²

Discussion

We first note that this is the most complex structure in terms of the number of constituent fragments that we have attempted to analyze, where the number of isotopic species we have used is less than the number of partial structure factors, although the number of structural parameters of the layer is also less than the number of partial structure factors. Judged by the self-consistency of the fits to the data the procedure seems to have been successful. While it is easy to justify such a procedure on fundamental grounds,¹² it is nevertheless important to show that it can be done in practice because it can greatly reduce the labor of preparing a large number of deuterated compounds and hence make the determination of the structure of adsorbed layers more accessible.

The structure is best represented in terms of the volume fraction profiles which are constructed by taking the number density profiles and multiplying them by the volume of each fragment. There is some uncertainty in the determination of the volume of each fraction. We have determined the volume of the *U* and *L* fragments using the standard parameters of Tanford,¹⁶ which give 250 Å³ for both *U* and *L* (2×125 Å³). The volume of the headgroup is estimated from the molecular

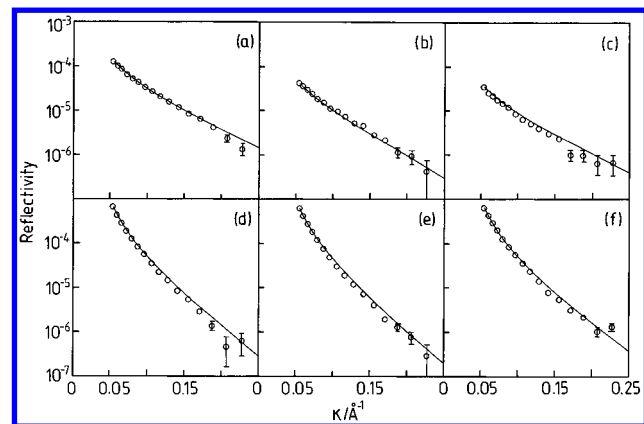
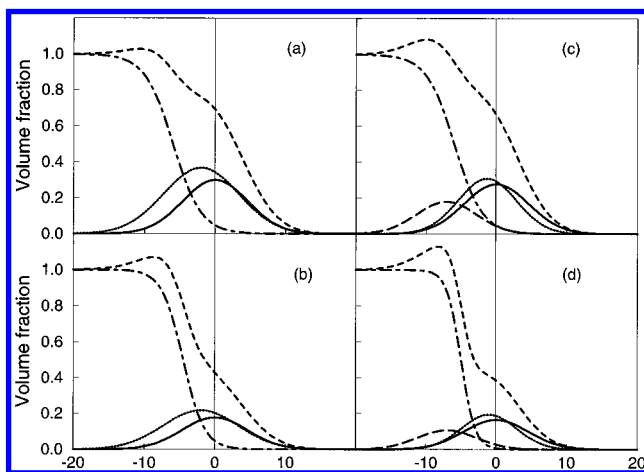
volume of 900 Å³, estimated from the density of solid AOT, less the volume of the two chains and that of a fully hydrated sodium ion of about 190 Å³. This leads to 210 Å³ for the headgroup, but there is considerable uncertainty in this value because it is sensitive to the state of hydration assumed for Na⁺ and SO₃⁻. The volume fraction profiles at the highest and lowest concentrations, cmc and cmc/300, are shown in Figure 5 using the subdivision of the AOT molecule into two and three groups. As already mentioned there is little difference in the structure of the AOT part of the layer for the two concentrations but the AOT layer as a whole shifts toward the underlying water at the lower concentrations. Also the *h* and *L* groups in the two representations are similar.

In general the values of the separations δ between the different fragments of the AOT molecule are expected to be independent of roughness, and they should therefore be the best basis for discussing the conformation of AOT at the interface. As we shall show below, this may not be the case for AOT but for the moment we interpret the parameters of Table 3 as if it were so. Table 3 shows that the separation between the centers of gravity of the butyl chain fragment and the remaining C₄H₈ fragment remains approximately constant at the small value of $1-1.5 \pm 1$ Å at all four concentrations studied. There are several possibilities for the conformation and orientation of the ethyl hexanol chain, which are shown in Figure 6. The hexane chain could be in the all-*trans* conformation, which would more or less ensure that this hexane fragment would lie horizontally on the surface (Figure 6c). Alternatively, the hexanol chain could be all-*trans*, in which case the ethyl group will be in a *gauche* conformation relative to the butyl group. The butyl group may then be oriented normal to the surface (Figure 6a) or so that both the ethyl and butyl groups are pointing as far away from the water as possible (Figure 6b). The all-*trans*-hexane chain (Figure 6c) is very unfavorable and the choice between Figure 6a and b will depend on exactly where the water surface lies with respect to the whole molecule. For the orientation in Figure 6a the distance between the center of gravity of the butyl chain and the remaining C₄H₈ fragment will be slightly more than the length of a C₂H₄ fragment, i.e., slightly larger than 2.6 Å. For the orientation in Figure 6b the separation will be about only 1.5 Å, which is close to the observed value. For the conformation in Figure 6b the mean position of the water surface, which is 6 Å from the center of the butyl chain is then approximately at the level of the oxygen atom in the ethyl hexanol, represented by the dashed line in the figure. This would mean that the headgroup of the AOT was very strongly immersed in the water, as the values of δ_{HW} in Table 3 suggest. The orientations of Figure 6a and b have the ethyl group quite close to the water surface, and the balance between the two conformations should be very sensitive to the degree of immersion of the molecule in the water. Table 3 shows that the only geometrical change of the layer with dilution of the surface is that the level of immersion of the molecule in the water increases, and it is therefore possible that the mean conformation of the chain changes in such a way that the intrinsic thickness of the layer actually increases as the coverage is reduced.

The width parameters, σ , of the layer, given in Table 3, suggest that the layer is rough. The maximum thickness that any of the fragments *U*, *L*, or *H* could have is approximately the length of a fully extended butyl chain, about 6 Å, which is considerably smaller than any of the observed values. Furthermore, this value is reduced to about 4 Å if the molecules are in the orientation of Figure 6b. As shown elsewhere¹⁷ the observed thickness σ is related to the roughness *w* of the whole layer

TABLE 3: Structural Parameters Obtained from the Kinematic Approximation When the Molecule Is Taken To Consist of Upper Chain (U), Lower Chain (L), and Head (H) Fragments

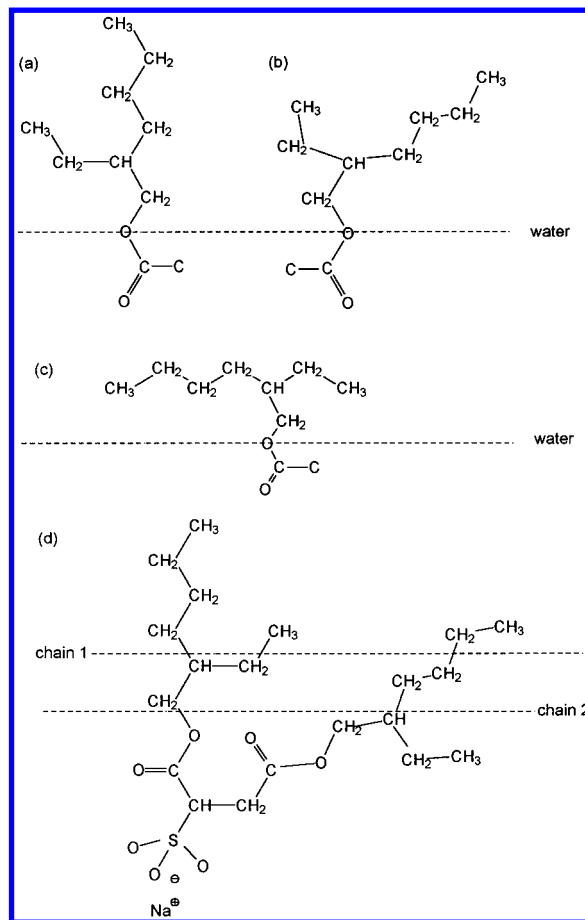
$A/\text{\AA}^2$	$\sigma_U \pm 1.5/\text{\AA}$	$\sigma_L \pm 1.5/\text{\AA}$	$\sigma_H \pm 2/\text{\AA}$	$\zeta \pm 1/\text{\AA}$	$\delta_{UW} \pm 0.5/\text{\AA}$	$\delta_{LW} \pm 0.5/\text{\AA}$	$\delta_{HW} \pm 1/\text{\AA}$
78 ± 2	13.0	11.5	12	4.0	6.0	4.5	-1.0
94 ± 3	13.0	11.5	12	3.5	5.5	4.5	-1.5
118 ± 4	13.0	11.0	12	3.0	5.5	4.0	-1.5
132 ± 5	13.0	11.0	12	2.0	5.0	4.0	-2.0

**Figure 4.** Best fits to reflectivity profiles from six out of seven different isotopic compositions of AOT at its cmc, (a) dUdL-AOT in NRW, (b) dUdL-AOT in NRW, (c) hUdL-AOT in NRW, (d) dUdL-AOT in D₂O, (e) dUdL-AOT in D₂O, and (f) hUdL-AOT in D₂O. The parameters used for the calculations are those in Table 3.**Figure 5.** Volume fraction profiles for the AOT monolayer at the air/solution interface at the cmc and at cmc/300. The volume fractions are given for both models used to analyze the data. In (a) and (b) the AOT molecule is divided into two (*U* and *h*) and in (c) and (d) it is divided into three fragments.

and the intrinsic dimension of the molecule along the surface normal direction l by

$$\sigma^2 = w^2 + l^2 \quad (12)$$

Taking the observed width of the butyl distribution of 13 Å and either of the intrinsic values of 6 or 4.5 Å given above leads to a value of w of 11.5–12 Å. A similar calculation using σ_L leads to a value of w of about 10.5 Å. Given the errors in the determination of the widths, we may conclude that the roughness of the layer at the cmc is 10–12 Å. If allowance is made for the contribution of capillary waves to this roughness, then the residual roughness is about 5 Å, which, given the nature of the errors in the quadrature formula (eq 12) should finally be taken to be between 0 and 6 Å. This is comparable with the values observed for non-ionic surfactants¹⁷ and considerably less than observed for single-chain ionic surfactants at their cmc (e.g., ref 18). However, if it is charge repulsion that causes the

**Figure 6.** Possible conformations and orientations of the ethyl hexanol fragment in AOT monolayers at the air/water interface. The dashed lines in (a), (b), and (c) represent the midplane of the water surface as determined from the parameters in Table 3 for the conformation in (b). The dashed lines in (d) indicate the approximate position of the centers of the two chain distributions.

intrinsic roughness, the surface charge density of an AOT layer is quite low and it may be insufficient to cause any additional roughness.

The widths of the distributions of the three fragments of AOT do not change as the coverage decreases. Since there is also little change in the δ values, this would imply that the overall roughness itself is also approximately invariant with coverage. However, the major contribution to the overall roughness comes from the capillary waves, and this contribution drops from a value of about 9.5 Å at the cmc to about 7 Å at cmc/300. This would mean that the non-capillary wave roughness actually increased as the coverage decreased, from 5 to about 10 Å. This not only is opposite to the behavior of all the surfactants we have so far studied but seems physically unreasonable. The only possible explanation is that the two chains in any given molecule are on average not at the same level. Thus the molecular conformation in Figure 6d would have a larger thickness than any single-chain surfactant. This type of disorder would also affect the values of δ in that the assumption that the δ s are decoupled from the roughness would no longer be valid. Thus, the conformation of Figure 6d, for example, would

reduce δ_{UH} and δ_{LH} but would not affect δ_{UL} . However, if these three parameters are constrained to be equal in the fitting procedure, as they are in the second of our fitting procedures, the fitted values of all three values of δ would be reduced and the apparent value of δ_{UL} would be less than its true value. If we make the assumption that, at the lowest surface coverage, roughness can only arise from capillary waves, or an average misorientation of the two chains within a single molecule, then, using 6 Å for the fully extended length of the butyl group, we conclude from the observed value of σ_U that the vertical displacement of the centers of the two butyl chains would have to have to be about 5 Å. This would imply considerable orientational disorder.

Schalchli et al.¹⁹ have done X-ray reflection experiments on the air/solution interface of AOT solutions and from black films of AOT. They obtained a very strange result at 0.5 cmc which indicated the presence of a film of material about 110 Å thick. A large spacing lamellar phase of AOT exists at higher concentrations, and we have observed this phase at the surface, but not until the concentration is more than 10 times the cmc.²⁰ The existence of any lamellar structure below the cmc is very unlikely, and the existence of a thick continuous film of AOT even less likely. AOT in aqueous solution undergoes a steady hydrolysis of the two ester linkages leading to the formation of the monoester, sodium sulfosuccinate, and ethylhexanol. Accumulation of a significant amount of ethylhexanol might lead to the formation of a partially wetting film at the surface, which could explain the observation of such a thick layer, but this would be difficult to prove one way or the other.

Finally, we compare the structure of the AOT layer at the air/liquid interface with that at the hydrophobic solid/liquid interface. The adsorption isotherms at the two interfaces are reasonably similar, as we have noted in a previous publication,³ but the AOT layer is significantly thinner at the solid/liquid interface. At this interface the chain (defined as $U + L$) thickness was found to be 9 ± 1 and the head thickness 7 ± 1 , where each layer was defined in terms of the uniform layer model. For comparison with Gaussian widths they should be multiplied by about 0.85 giving 8 and 6 Å, respectively, to be compared with about 15 and 11 Å at the air/liquid interface. If

we remove the contribution of capillary waves to the latter using eq 12, we obtain about 11 Å for the chain and 0–6 Å for the heads. While the agreement is not particularly good, it does indicate that the AOT layer at the solid/liquid interface is similar to that at the air/liquid once capillary wave roughness is removed, i.e., the two layers are similar on the short-range lateral scale.

Acknowledgment. We thank the EPSRC for support for this work. Z.X.L. thanks the British Council for a grant.

References and Notes

- (1) Porter, M. R. *Handbook of Surfactants*, 2nd ed.; Blackie: London, 1994.
- (2) Li, Z. X.; Lu, J. R.; Thomas, R. K.; Penfold, J. *Prog. Colloid Polym. Sci.* **1995**, 98, 243.
- (3) Fragneto, G.; Li, Z. X.; Thomas, R. K.; Rennie, A. R.; Penfold, J. *Colloid Interface Sci.* **1996**, 178, 531.
- (4) Lu, J. R.; Smallwood, J. A.; Thomas, R. K.; Penfold, J. *Phys. Chem.* **1995**, 99, 8233.
- (5) Li, Z. X.; Lu, J. R.; Thomas, R. K. *Langmuir*, submitted.
- (6) Furniss, B.; Hannaford, A. J.; Smith, P. W. G.; Tatchell, A. R. *Vogel's Practical Organic Chemistry*, 5th ed., 1989.
- (7) Jaeger, A. O. U.S. Patent 2028091, 1936.
- (8) Williams, E. F.; Woodberry, N. T.; Dixon, J. K. *J. Colloid Interface Sci.* **1957**, 12, 452.
- (9) Mukerjee, P.; Mysels, K. J. *Critical Micelle Concentrations of Aqueous Surfactant Systems*; NSRDS-NBS 36, 1971.
- (10) Lee, E. M.; Thomas, R. K.; Penfold, J.; Ward, R. C. *J. Phys. Chem.* **1989**, 93, 381.
- (11) Born, M.; Wolf, E. *Principles of Optics*; Pergamon: Oxford, 1970.
- (12) Lu, J. R.; Lee, E. M.; Thomas, R. K. *Acta Crystallogr.* **1996**, A52, 11.
- (13) Simister, E. A.; Lee, E. M.; Thomas, R. K.; Penfold, J. *J. Phys. Chem.* **1992**, 96, 1373.
- (14) Simister, E. A.; Lee, E. M.; Thomas, R. K.; Penfold, J. *Macromol. Rep.* **1992**, A29, 155.
- (15) Lee, E. M.; Milnes, J. S. *J. Appl. Crystallogr.* **1995**, 28, 518.
- (16) Tanford, C. J. *J. Phys. Chem.* **1972**, 76, 3020.
- (17) Lu, J. R.; Hromadova, M.; Thomas, R. K.; Penfold, J. *Langmuir* **1993**, 9, 2417.
- (18) Lu, J. R.; Hromadova, M.; Simister, E. A.; Thomas, R. K.; Penfold, J. *J. Phys. Chem.* **1994**, 98, 11519.
- (19) Schalchli, A.; Sentenac, D.; Benattar, J. J.; Bergeron, V. *J. Chem. Soc., Faraday Trans.* **1996**, 92, 553.
- (20) Li, Z. X.; Lu, J. R.; Thomas, R. K.; Penfold, J. *J. Chem. Soc., Faraday Trans.*, in press.